JOURNAL OF MATERIALS SCIENCE **39** (2004) 867–879

Potential for integration of electrophoretic deposition into electronic device manufacture; demonstrations using silver/palladium

J. VAN TASSEL, C. A. RANDALL
Materials Research Institute, The Pennsylvania State University, University Park, PA 16801, USA
E-mail: vantassel@psu.edu
E-mail: car4@psu.edu

A silver palladium (Ag/Pd) alloy powder is used as an example material to illustrate potential applications of electrophoretic deposition (EPD) in electronics manufacturing, in particular the forming of multilayer devices. The dispersion and deposition of the Ag/Pd powder in acetic acid is characterized. It is found that deposition can be explained by the direct action of electrostatic force on individual particles. Depositions of this Ag/Pd powder are then used to demonstrate: forming of a continuous layer on a rigid substrate; forming of continuous layers in laminated and sintered $BaTiO_3$ multilayers; and incorporation of patterned depositions into a multilayer by either overcasting the patterned deposition with a particulate slip to form a multicomponent tape, or direct lamination of the patterned deposition to a low temperature co-fired ceramic (LTCC) tape. It is shown that electrically conducting layers can be formed at an average thickness of only two times the diameter of the starting powder. Continuous conductor lines thirty times the average diameter of the starting powder were formed.

1. Introduction

For nearly fifty years multilayer ceramic structures have been fabricated by casting a continuous ceramic tape, screen printing a patterned electrode layer onto the tape, stacking the tape layers and lamination of these multicomponent tapes. This is followed by de-binding and sintering to form devices such as multilayer ceramic capacitors and multilayer co-fired ceramic (MLCC) substrates and wiring modules. As with all electronic devices, there is continuous pressure to reduce device sizes and increase volumetric efficiency. The state of the art is being pushed fastest in the multilayer capacitor industry where commercial devices currently available have 2 μm dielectric layers separating 0.5 μm electrode layers, with the near term target to reduce these thicknesses to one micron and a few hundred nanometers respectively. Aiding this drive to sub-micron feature sizes is an increasing availability of ceramic and metal powders in the nanometer size range. It is unclear at this point if tape casting and screen printing will be able to take advantage of these nano powders to produce the sub-micron features necessary for future devices. It is therefore important to consider and demonstrate new methods to take particulate processing into the nanoparticle age.

Traditional manufacturing processes use mechanical devices to manipulate particles as slurries or inks; e.g., a doctor blade in tape casting or a squeegee and patterned screen in screen printing. The minimum scale for these processes is the scale at which the slurry, slip or ink can be treated as a continuous medium. In contrast, EPD uses electric fields to act directly on the particles, moving them to the desired location independent of the suspending solution. The minimum scale for EPD is therefore the size of the individual particles. This means that EPD can take maximum advantage of reduced particulate sizes to produce the minimum thickness and feature sizes possible from a given particulate size starting material. This makes EPD an interesting alternative technology for handling the very fine powders and producing the very thin layers that will be necessary to advance ceramic particulate technology into the future.

However, EPD is not a technology confined only to the very small. EPD can manipulate particles from a few nanometers to several microns to produce objects and coatings from nanometers to centimeters. Fig. 1 compares various production technologies. Of these technologies EPD has the widest dimensional range—from nanometer scale with field assisted self assembled structures, through to centimeter scale electrolyte ceramics [1, 2].

There are three basic steps involved in EPD. The first step is to create a stable, charged suspension of the particles to be formed. For the suspension to be stable there must be an interparticle repulsive force preventing the particles from coming into range of the London-Van der Waals (L-VdW) attractive force, which would cause the particles to agglomerate in low density flocs

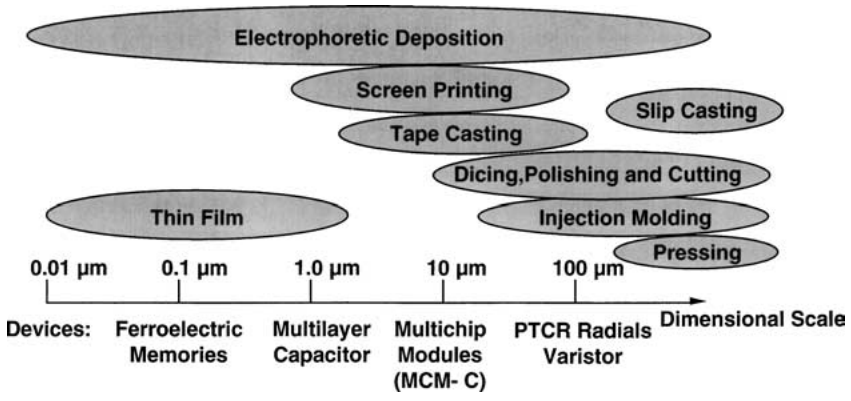

Figure 1 Thickness ranges of applicability for various production technologies.

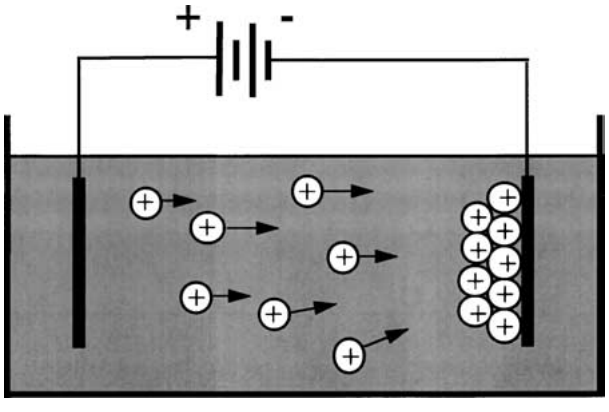

Figure 2 Positively charged particles will migrate to, and can be made to deposit on, a negatively charged electrode.

and rapidly sediment out of the working suspension. The particle surface is chemically given an electrostatic charge so that the particles can be moved by an applied electric field.

The second step is to apply an electric field across the suspension, causing the charged particles to migrate toward the oppositely charged electrode where they will accumulate. This process is shown schematically in Fig. 2.

Finally, at the deposition electrode the particles are brought into contact with each other and the deposition electrode allowing the L-VdW force to hold the particles together in a rigid deposition. For this contact to occur the force keeping the particles separated in bulk suspension must be overcome. A conducting electrode creates a complex and usually non-equilibrium electrochemical environment in the fluid layer adjacent to its surface. This means that there are a variety of effects which can act to reduce, eliminate or overcome the mechanism used to stabilize the particles in the bulk.

For the demonstration in this paper, we have selected an EPD system with minimal accompanying electrolytic conduction. While this does not eliminate electrochemical effects, our analysis of the particles' electrostatic stabilizing force suggest that in this case deposition can be explained by the simple electrostatic force on a charged particle in the applied electric field.

This, arguably the simplest of the EPD mechanisms, allows particles to be brought into the deposition uniformly from their random distribution in the bulk suspension. The random addition of individual particles to the deposition allows the formation of extremely uniform thin particulate layers. As is shown below, layers of particles deposited by EPD only two to three particle diameters thick can be consolidated and sintered to form dense, continuous layers in a multilayer structure.

Excellent reviews covering much of the published literature on EPD have been published by Sarkar and Nicholson [3], Gani [4], and most recently Boccaccini and Zhitomirsky [5]. The objective of this article is to outline some of the technical advantages and challenges for the integration of EPD into the manufacture of multilayer electronic devices.

2. Materials

2.1. Deposited powder

The powder used is a 70/30 alloyed silver/palladium composition (EGAG07001 from PGP Industries, Inc. Santa Fe Springs, California.) The particles are spherical with an average diameter of 0.3 μm as determined by light scattering (MasterSizer, Malvern Instruments, United Kingdom). The surface area is 1.73 m^2/g as determined by single point BET (Monosorb MS-12, Quantachrome) giving an equivalent surface area diameter of 0.32 μm.

2.2. Acetic acid

J. T. Baker glacial acetic acid, 99.5–100.5% (J. T. Baker Co., Phillipsburg, New Jersey) was used as the suspending solvent.

2.3. Deposition substrates

Deposition was conducted onto three types of substrates—Pre-sintered alumina substrates (Superstrate 996, Coors Ceramics Co., Golden, CO), glass, and polyester film. The conductive deposition electrode on all three substrates was created by a sputtered platinum coating of ≈40 nm thickness. Patterns on glass substrates were created by scribing a continuous coating. Patterns on polyester film substrates were created using an UV-photolithographic mask on the film surface.

2.4. Pre-formed ceramic tapes

Laminations were carried out on pre-formed ceramic tapes. These include a commercially produced tape, DuPont LTCC tape 951-A, and tapes made in-house by

Bi-coating Cabot hydrothermal $BaTiO_3$ powder (BT-8, Cabot Performance Materials, Boyertown, PA) [6], and mixing the powder with binder and solvent to form a slip, which was cast into tape by traditional methods.

3. Experimental procedure

3.1. Suspension

Suspensions were produced by the addition of 1.0 g of powder to approximately 100 g of glacial acetic acid having a conductivity of less than 0.03 μS/cm prior to the addition of the powder. The powder was then dispersed by sonication using a Branson Sonifier 350 at 70% setting for two minutes while stirring.

3.2. Mobility

Mobility was measured using a Delsa 440 laser Doppler velocimeter (Beckman Coulter, Inc., Fullerton, California). This instrument measures particle velocity in suspension within a rectangular capillary measuring 0.98 mm high, 3.17 mm wide, and 5.18 mm long. To separate the electro-osmotic flow of the fluid in the capillary from the electrophoretic motion of the particles, particle velocity was measured at nine points across the capillary, the results fitted to a parabola, and the particle velocities at the theoretical stationary levels calculated from the fitted parabola. The theoretical stationary layers at the center of the width of this capillary occur at 16% of the capillary height away from the top and bottom of the capillary. This is similar to the procedure outlined by Pelton *et al*. [7].

The measurement for each point from top to bottom of the capillary consisted of applying a constant voltage in one direction for two seconds, a one second interval, followed by application of the voltage in the opposite direction for two seconds. This is repeated for a total of 30 s. This is intended to minimize the voltage drop due to electrochemical polarization at the electrodes.

For a significant signal to be generated by the instrument the laser must be able to propagate across the capillary with only modest scattering. This requires that the sample have a volume density of particles in suspension of approximately 0.01%, one tenth the volume density of the deposition suspensions used here. To prepare these dilutions the suspension was allowed to sediment overnight yielding a clear supernatant. Some of this supernatant was removed, the particles re-suspended, and the suspension and supernatant mixed to yield the appropriate suspension density for measurement.

3.3. Conductivity

Conductivity was measured using an open sided, rectangular, parallel plate conductivity cell having a cell constant of 0.107 cm^{-1} (Thermo Orion, Beverly, Massachusetts). The voltage across the conductivity cell was measured using a voltage divider circuit. A sine wave input signal of $\approx$1 V rms at 10 Hz was provided by an HP 33120A signal generator. The voltage across the conductivity cell was reduced to $\approx$0.5 V rms using a resistance decade box. The total input voltage and voltage across the decade box were measured using an HP 54645A oscilloscope and used to calculate the resistance across the conductivity cell. This setup was calibrated over the range from 1 to 60 μS/cm by titration of KCl in water using the equation of Lind *et al*. [8] as standard.

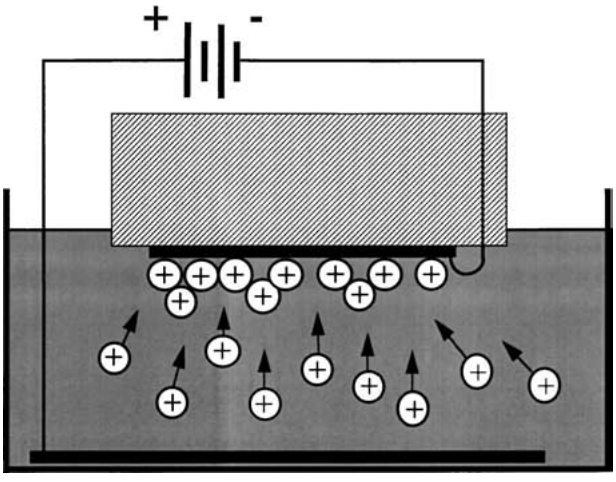

Figure 3 Upward deposition separates EPD from sedimentation.

3.4. Deposition

The powder was deposited onto a platinum electrode surface sputtered onto either a glass plate, for the overcasting demonstration, or onto 2.54 cm square pieces of uncoated polyester film tape casting carrier for the lamination demonstrations. The suspension was placed in a beaker with a gold foil in the bottom to serve as the anode. The deposition surface is held horizontally one half, one or two centimeters above the anode. The particles are then deposited vertically upward to get a deposition that is only due to electrophoretic effects without sedimentation components. This is shown schematically in Fig. 3.

To deposit the particles an electric field of $\approx$300 V/cm was applied. For the thinnest depositions the field was pulsed on and off in three or five second intervals to allow electroconvective circulation to dissipate. This was done to maximize the thickness uniformity of these very thin depositions. After deposition was complete, the substrate was removed from the holder and immediately rinsed by dipping and moving back and forth gently in as-received acetic acid. This is to remove any particles which are not deposited but are carried out of the deposition bath in the wetting film of acetic acid on the deposition surface.

4. Dispersion and deposition results and discussion

4.1. Electrophoretic mobility

Several mobility measurements were made at voltage settings of 15, 30, 45, and 60 V. The measured mobility increased linearly by $\approx$20% from 15 to 60 V. This is presumably due to electrode polarization and therefore the mobility at the highest voltage was taken as the most accurate. One measurement at 60 V is shown in Fig. 4.

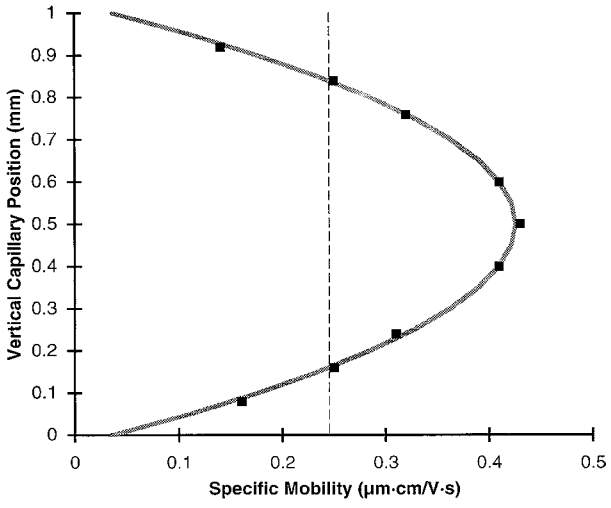

Figure 4 Specific mobility vs. vertical position in measurement capillary. The vertical dashed line intersects the parabola at the theoretical stationary layers.

The parabola was fitted to the data by least squares. The r^2 fit of the parabola was 0.996. The mobility at the theoretical stationary levels is 0.25 μm · cm/V · s. Reproducibility of measurements was ± 5%. Suspensions with the conductivity reduced by dilution with fresh acetic acid had a mobility ≈10% less than the suspensions diluted only with suspension supernatant. Mobilities in the freshly prepared suspension and in the suspension after a series of depositions were estimated at 0.23 and 0.25 μm · cm/V · s respectively.

4.2. Conductivity and ionic strength

The conductivity of one typical suspension after sonication was 0.04 μS/cm. This conductivity increased with each deposition, presumably due to the electrolytic formation of ionizable species during conduction. After a total current flux through the suspension of 80 mC over the course of eighteen depositions the conductivity was 0.11 μS/cm. The conductivity measurements were reproducible within ±0.01 μS/cm, however, absent standardization for the range below 1 μS/cm, the absolute conductivity values here should be considered only approximate. Based on prior experience we believe that the measured values will be within a factor of two of the actual values.

In order to estimate the ionic content of the suspension without knowing the specific ionic species leading to conduction, it is necessary to make some assumptions. First, due to the low dielectric constant of acetic acid, it is assumed that any free ions will be univalent. Second, an approximate molar conductivity of 6 μScm^{-1} mMolar^{-1} is chosen. This number is based on the work of B. V. Weidner who measured molar limit conductivities of various ammonium and nitrate salts ranging from 5 to 8 in pure acetic acid [9]. Using this value for the ionic molar conductivity it is possible to estimate the ionic content of the suspension as ranging from 6 μMolar before deposition, rising to 18 μMolar after a series of depositions.

In this series of eighteen depositions averaging twenty seconds each, a total current of 80 mC passed through the suspension. If the conduction does occur by an electrolytic process which produces an ion pair for each electron passing through the solution, this current would result in an increase of ionic content of 9 μMolar in the 90 cc of this suspension. This is well within the error limits of the 12 μMolar rise in the ionic concentration estimated by conductivity. Therefore, this hypothesis cannot be rejected.

With an estimate for the ionic strength of the solution it is now possible to calculate the inverse Debye length using formula (1) for a solution containing univalent ions. (symbols used are defined in appendix.)

$$\kappa = \left[\frac{2e^2\rho_\infty}{\varepsilon_o\varepsilon_r kT}\right]^{\frac{1}{2}} \quad \text{Inverse Debye Length} \qquad (1)$$

Ionic concentrations in the bulk solution, c of 6 and 18 μMolar will yield Debye lengths, κ^{-1}, of 35 and 20 nm in acetic acid with a relative dielectric constant, ε_r, of 6.2. For the 300 nm particles used here this yields non-dimensional double layer thickness parameters, κa, of 4.3 and 7.5.

4.3. Surface potential and surface charge

With the particle electrophoretic mobility and the double layer thickness parameter it is possible to estimate the zeta potential of the particle. Unfortunately, the κa values here are within the range of 1–10 where the simple Hückel and Smoluchowski formulae are not valid, and the non-dimensional electrophoretic mobility values, **E**, are 2.6 and 2.8, well outside of the 0 to 1 range for validity of the slightly more complex Henry formulation [10].

$$\mathbf{E} = \frac{3\eta e}{2\varepsilon_r\varepsilon_o kT}u_E \qquad (2)$$

Non-dimensional Electrophoretic Mobility

Therefore to estimate the surface potential, graphic interpolation of the charts published by O'Brien and White was used [11]. These calculations include the retardation due to polarization of the diffuse layer around the particle. These charts were calculated on the basis of KCl in water, where the ionic mobility is much higher than in the acetic acid suspension used here. The boundary layer polarization is likely to be higher in the suspension with the lower ionic mobility, leading to an under estimate of the actual surface potential. For $\mathbf{E} = 2.6$ and 2.8, and κa's of 4.3 and 7.5, the non-dimensional surface potentials, $\tilde{\zeta}$, are both 3.0. This yields a constant surface potential of 77 mV independent of the solution ionic concentration.

$$\tilde{\zeta} = \frac{e\zeta}{kT} \quad \text{Non-dimensional Surface Potential} \qquad (3)$$

With the surface potential and κa, the surface charge density can be calculated using the empirical formula of Loeb *et al.* [12] for a 1-1 electrolyte system, Equation 4. This gives a particle surface charge density, q, of 0.20 and 0.32 milliCoulombs/meter^2 for the 6 and

18 μMolar suspensions respectively. For the 300 nm particles used here, this gives total particle charges of 5.5×10^{-17} and 9.1×10^{-17} Coulombs.

$$q = \frac{\varepsilon_o \varepsilon_r kT}{e} \kappa \left(2 \sinh \left(\frac{1}{2} \tilde{\zeta} \right) + \frac{4}{\kappa a} \tanh \left(\frac{1}{4} \tilde{\zeta} \right) \right) \quad (4)$$

Surface Charge Density

4.4. Stability

To prevent the particles from floccing and sedimenting out of the suspension prior to deposition there must be an adequate force to keep them apart. The force drawing them together is, of course, the London-Van der Waals force and, in this case, the force that must overcome this attraction is the increased osmotic pressure due to the compression/overlap of the particles' diffuse counter-ion layers.

The L-VdW attraction between two particles is the product of two terms. The Hamaker Constant, which is a function of the electronic properties of the materials, and a geometric term defined by the arrangement of the materials. This is expressed in Equation 5 where A_{131} is the Hamaker constant and the balance is the geometric factor for spheres of radius a at a center to center separation distance of r [13].

$$\Phi = -A_{131} \frac{1}{6} \left(\frac{2a^2}{r^2 - 4a^2} + \frac{2a^2}{r^2} + \ln \frac{r^2 - 4a^2}{r^2} \right) \quad (5)$$

L-VdW Interaction Energy for Two Spheres

For the Hamaker constant at zero separation we have used the value calculated by Parsegian and Weiss [14] for two masses of silver metal separated by water, $A_{131}(0) = 4.0 \times 10^{-19}$ Joule. Given that silver and palladium form a full solid solution, it is reasonable to expect that the electronic properties of silver palladium will be similar to those of pure silver. Likewise, the close match of the optical frequency refractive indices for water and acetic acid, at 1.333 and 1.372 respectively, indicate that they will likely have a similar dielectric relaxation behavior in the UV range where all of the interaction takes place. These assumptions are supported by the approximation methods of Israelachvilli and their comparison to experimental values [15].

The Hamaker constant itself is a function of separation distance. The synchronization of dipole motions that leads to the London electrostatic attraction decays as the separation approaches a significant fraction of the length of the electromagnetic wave mediating this interaction. For the silver palladium particles here the interaction will be in the plasmon frequency range, $\approx 3 \times 10^{15}$ s^{-1}, with a wavelength of 100 nm. This retardation effect leads to a decrease in the effective Hamaker constant by 50% at a separation distance of 10 nm and with the interaction almost completely disappearing at 100 nm. This retardation was calculated here using the method of Russel *et al.* [13].

The repulsive force was then calculated using the linearized Derjaguin approximation for two spheres at constant surface potential (6) [13].

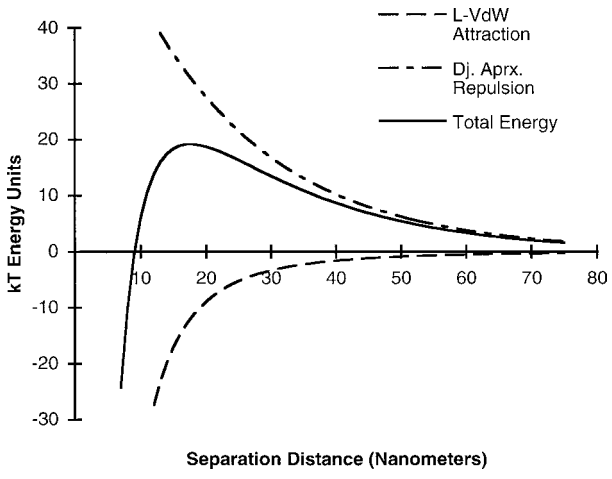

Figure 5 Interaction potential for two 300 nm dia. silver palladium spheres in acetic acid; $c = 18$ μMol.; $y_o = 77$ mV.

$$\Phi = 2\pi \varepsilon_r \varepsilon_o \zeta^2 a \ln(1 + e^{-\kappa h}) \quad (6)$$

Derjaguin Approx. Repulsion Energy

Summing the L-VdW and electrostatic interaction potentials gives the total interaction energy. This is shown in Fig. 5 for the particles at the higher ionic strength condition. The calculated energy barriers to flocculation are 33 and 19 kT energy units and the maximum repulsion forces are 2.6×10^{-12} N and 2.3×10^{-12} N for the 6 and 18 μMolar conditions respectively.

For the surface potentials found here, the linearization assumption in the Derjaguin approximation (6) of the electrostatic force will lead to an underestimation of the potential drop near the particle surface and therefore an overestimation of the energy barrier to flocculation and interparticle repulsive force. This may, at least in part, be compensated by the likely underestimation of the surface potential above.

4.5. Deposition

With the maximum interparticle force and total particle charge it is possible to calculate the voltage gradient that would produce a force on the particle equal to the maximum interparticle repulsive force. This works out to voltage gradients of 470 and 250 V/cm for the 6 and 18 μMolar cases respectively. Given the uncertainty in the measurement and calculation of the interparticle potential, this result is in good agreement with the observed voltage gradient necessary for deposition of 300 V/cm.

Based on the above analysis it is reasonable to believe that deposition of the particles in this case occurs primarily by electrostatic force on individual particles.

5. Demonstrations of the integration of EPD in electronics fabrication

5.1. Uniform coatings on a rigid substrate

A very common operation in electronic manufacturing is the formation of a uniform metallic coating. These are formed by sputtering, screen printing, electroplating

and electroless plating. They are sometimes used as a continuous layer for a ground plane or electronic shielding. Very frequently these continuous layers are masked and etched to produce circuit patterns. Here the objective was to produce an electrode which would be stable and compatible as a bottom electrode for an EPD formed PZT layer to be sintered at 850°C [16].

Demonstration

Shown in Fig. 6 below is a one micron layer of silver/palladium that was formed by EPD onto a standard alumina circuit substrate and sintering of the deposition. The substrate was prepared by sputtering of a 40 nm platinum coating to make the surface conductive. The electrode spacing was 2 cm, 500 V was applied for 45 s generating a current of 42 μA/cm^2. After rinsing the dried deposition weight was 1.0 mg/cm^2. The deposition was densified by heating in air to 900°C at 15°C/min and allowing to cool at a maximum 15°C/min. The resulting coating was uniform, adherent and examination by SEM revealed no through thickness pores greater than 1 μm.

To create a film of this thickness by sputtering would take as much as an hour. To produce a one micron coating of a single metal such as copper by electrodeposition would take only a little longer than electrophoretic deposition and would not need a sintering step to densify

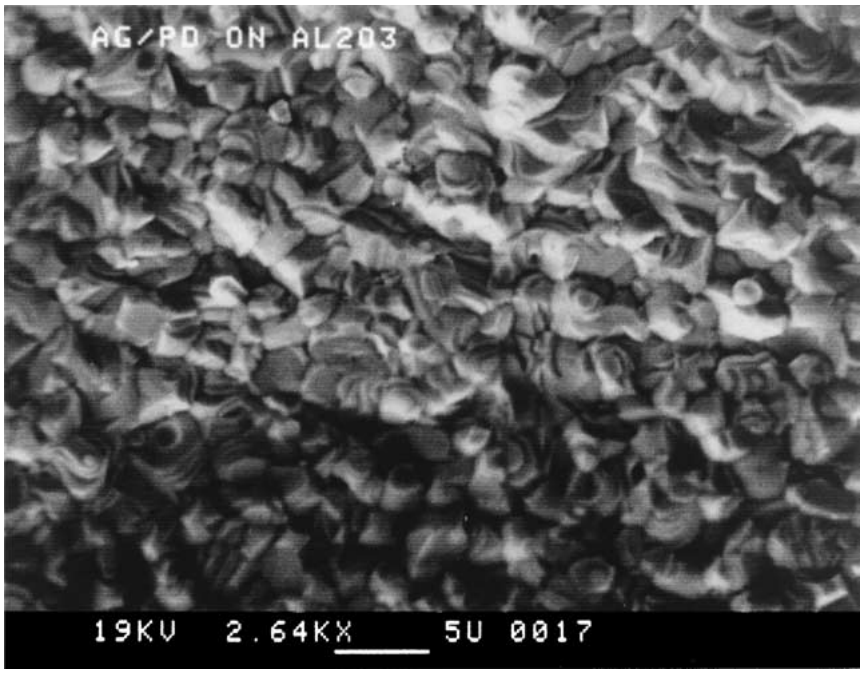

(a)

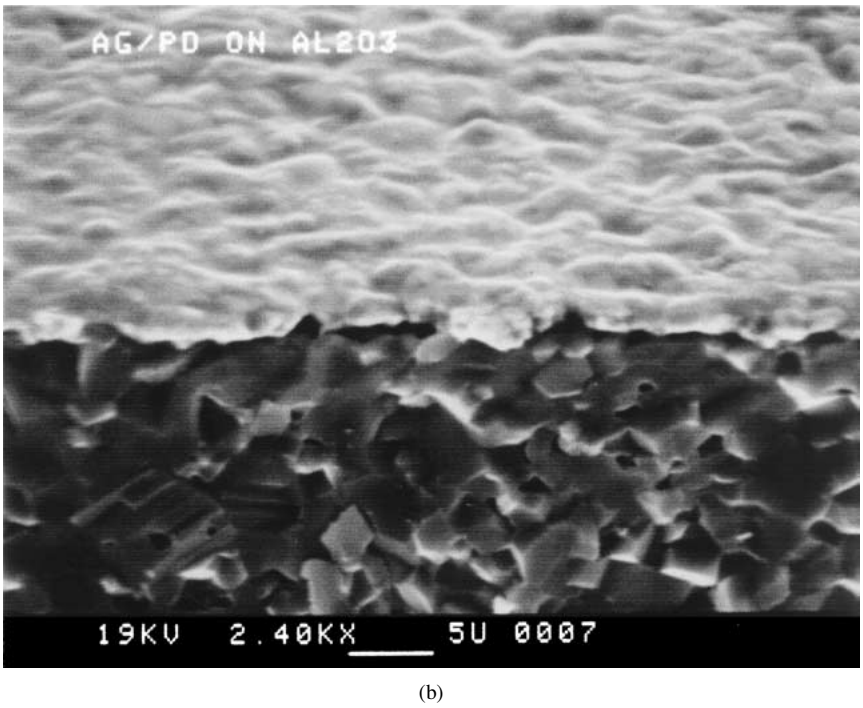

(b)

Figure 6 One micron thick Ag/Pd layer on an alumina circuit substrate, (a) top view, (b) oblique view of fracture edge, Ag/Pd on top, fracture surface of substrate below.

the coating, however, forming a coating of an alloyed metal by electrodeposition is a much more difficult and involved process when it is possible at all. Screen printing can rapidly create a coating of an alloyed powder, but cannot produce a uniform continuous coating at this thickness on a rigid substrate. EPD is unique in being able to produce a controlled stoichiometry alloy layer rapidly and inexpensively in the one micron thickness range.

5.2. Use of EPD in multilayer fabrication

While EPD may have advantages for the production of continuous coatings in certain cases of electronics manufacturing, it is in multilayer electronic device fabrication where EPD has the potential to dramatically improve the state of the art.

The current standard technology for production of multilayer electronic devices consists of: (1) casting of a continuous dielectric particulate tape layer, (2) punching and filling of vias through the continuous tape to provide interconnection between layers, and (3) screen printing patterns of conductor, resistor, inductor and capacitor materials onto the continuous tape. These multicomponent tapes are then stacked, laminated under pressure to fuse the layers together, and sintered to form the final device.

EPD has the potential to reduce the scale of these multicomponent tapes by an order of magnitude over current technology both in thickness and lateral dimensions, improve the uniformity the final device, and remain cost competitive with current high volume production techniques. The demonstrations below cover the forming of continuous layers, forming of a continuous thickness multicomponent tape, creation of micron scale patterns, and a discussion of the forming of multicomponent tapes completely by EPD.

5.2.1. Forming continuous layers for multilayer devices

The simplest application of EPD is in the creation of uniform thickness tapes, such as are currently produced by doctor blade tape casting. To do this the entire tape carrier is coated with a conductive layer. A voltage is applied to the carrier in a deposition bath and a uniform layer of the particulate material is deposited. Binder can either be dissolved in the solvent for the EPD bath or can be introduced into the tape in a second step.

The advantage of this process is the formation of a tape with more uniform particle packing than can be achieved by traditional tape casting. This in turn should lead to the ability to create uniform tapes that are significantly thinner than is currently possible. This is thinner both in absolute terms and in terms of the number of average particle diameters, i.e., thinner tapes could be created with the same size particles without loss of continuity.

Demonstration

The objective of this experiment was to determine the minimum thickness continuous electrode layer that could be formed using the 0.3 μm Ag/Pd powder. Multilayer stacks were built up layer by layer with each layer handled on a polyester film carrier until it was laminated to the stack and the carrier peeled off.

The barium titanate layers were formed by screen printing onto a polyester carrier film. The screen printing ink was prepared using a standard tape casting binder (Ferro B73210) to allow for lamination of the films. The barium titanate powder used was Cabot BT-8 coated with 5 wt% bismuth oxide to promote sintering in the 700–800°C range. The BT-8 average particle size is 0.2 μm with a generally smooth, equiaxed particle shape. A 2.54 cm square pattern was printed through a 10 μm thick screen and was dried at 80°C yielding a 2 to 4 μm thick tape layer.

The silver/palladium was deposited onto 2.54 cm square pieces of polyester film with a sputtered platinum layer to make the deposition side conductive. A deposition voltage of 200 V/cm was applied 5 s on, 5 s off, for a period of 90 s (45 s on). No binder was added to the silver palladium layers prior to lamination.

Lamination was performed in a heated, uniaxial lamination press at 40 MPa and 70°C. The silver/palladium deposition was placed face down onto a barium titanate layer and pressed. Under these conditions there was enough diffusion of binder from the barium titanate layer into the metal powder to bond it to the stack. The platinum sputtered polyester could be peeled off the stack leaving all of the silver-palladium powder laminated to the layer below. The polyester retained its shiny conductive surface and could be used again for another deposition. A barium titanate layer was then laminated on top of the metal layer and the process repeated.

The results of the first laminate produced are shown in Fig. 7 below. The green cross section Fig. 7a shows the Ag/Pd powder layer that when sintered yields one of the 1.2 μm layers shown in Fig. 7b. The polished cross section examined in the SEM was 5 mm wide. The picture in Fig. 7b is representative of the uniformity of the Ag/Pd layers over the entire width of the specimen. No pores or gaps were seen over the 5 mm examined.

The continuity and uniformity of these 1.2 μm layers are representative of what would be required of a dielectric layer. An electrode layer can have a significant number of through thickness pores while still maintaining electrical continuity. Based on the multilayer above it appeared that the electrode thickness could be reduced by half without losing continuity. To test this a second multilayer was made using depositions of Ag/Pd powder one half the thickness used in the first example. The depositions were formed using 200 V/cm applied continuously for 15 s. The resulting multilayer is shown in Fig. 8.

The silver/palladium layers formed averaged 0.6 μm thick and were continuous across the width of the 5 mm sample prepared. Examination of the full 5 mm width of the polished cross section in the SEM showed very few pores that extended through the 0.6 μm layer.

What has been demonstrated here are the likely minimum thicknesses possible for two types of layers formed by EPD of equiaxed particles. For dielectric or membrane layers where there should be no through

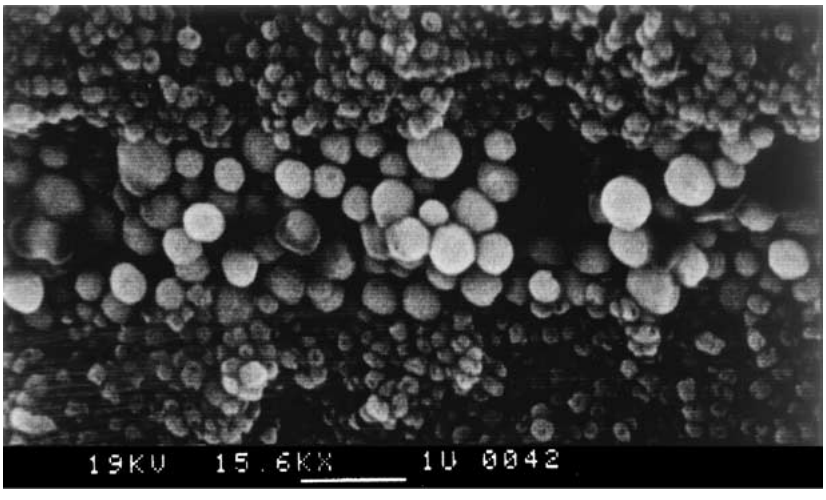

(a)

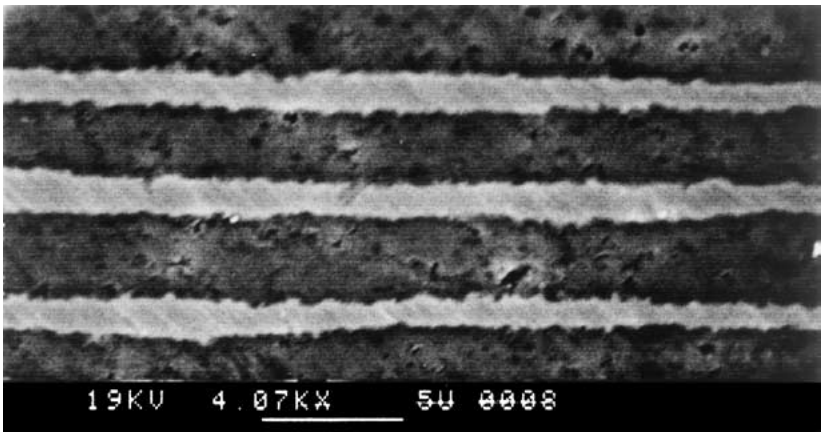

(b)

Figure 7 (a) Green cross section showing Ag/Pd powder layer (center) between barium titanate layers (top & bottom); (b) Polished cross section of sintered multilayer showing 1.2 μm thick Ag/Pd electrode layers (light color layers) between 2.5 μm layers of barium titanate.

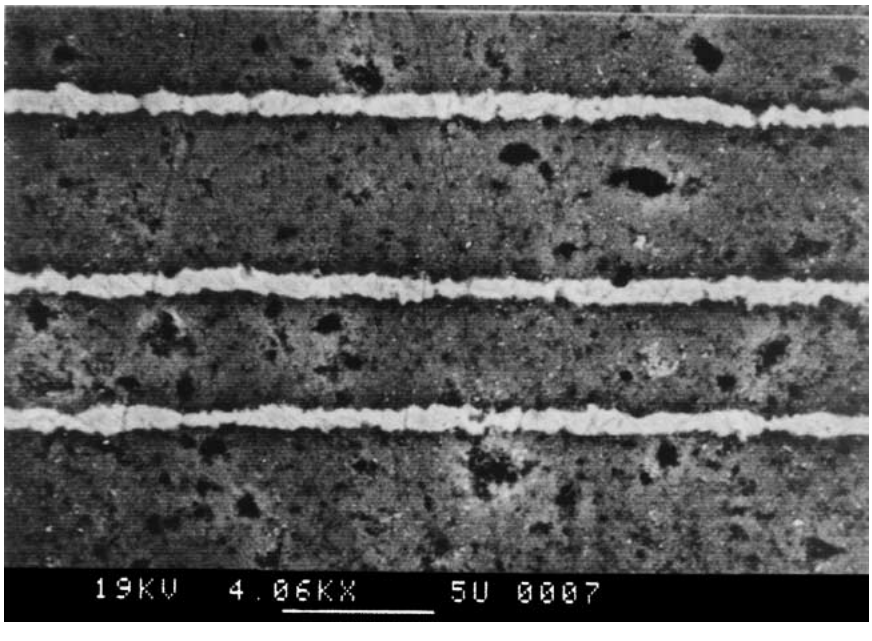

Figure 8 Polished cross section of sintered multilayer showing 0.6 μm thick Ag/Pd electrode layers (light colored layers).

thickness pores or areas of significantly reduced thickness, the minimum thickness will be 4–5 times the average particle diameter. This corresponds to the four particle diameter thick layers in Fig. 7. For capacitor electrodes, ground planes or shielding layers it is only necessary to maintain connectivity in the plane of the electrode and significant through thickness porosity can be tolerated. Here the minimum thickness will be $\approx$2 times the average starting particle diameter. Prior experience in this lab at forming 50 nm thick layers by

EPD of 10 nm diameter silver particles [17] strongly suggests that this thickness scaling based on average particle diameter will be valid throughout the nanometer region as well. By moving to the EPD of nanoparticles it should be possible to rapidly and inexpensively produce layer thicknesses that have previously only been possible using traditional thin film processes.

5.2.2. Tape overcasting on EPD patterns

Another application of EPD is to combine it with traditional doctor blade tape casting to produce a uniform thickness multicomponent particulate tape. By applying a voltage to a conductive pattern on the tape carrier, one type of particulate material can be deposited in that pattern onto the carrier. With multiple patterns more than one material could be deposited. This is followed by normal tape casting of the final material over the deposited components. The solvent containing the binder from the tape casting slip will impregnate the electrophoretically deposited components, incorporating them into the tape. By this means a uniform thickness tape can be produced that incorporates secondary materials for conductors, resistors, capacitors, etc. This is shown schematically in Fig. 9.

The advantage of this process is that it creates a uniform thickness multicomponent tape. In the traditional process a uniform thickness tape is cast and secondary components are screen printed onto the surface of this tape, making the thickness of the multicomponent tape uneven. When many of these tapes are stacked, low density areas can be left in the laminate, as illustrated in Fig. 10a. These cause stress concentrations which can serve as failure origins in sintering or use of the device.

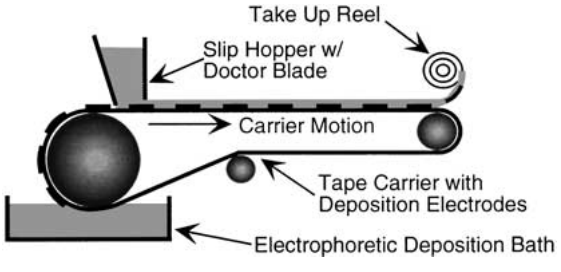

Figure 9 Combining EPD on a tape carrier with tape casting can be used to create a uniform thickness, multicomponent particulate tape.

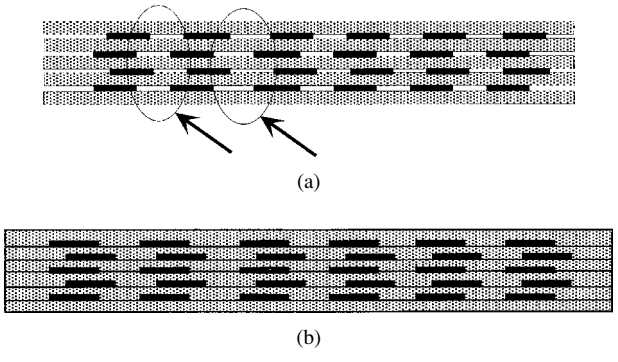

Figure 10 (a) Uneven thickness leads to low density regions and (b) Laminate of even thickness tapes eliminates low density regions in green body.

The key to this process is the thickness uniformity of the layers formed by EPD. This would allow a much thinner layer of material to be tape cast over the components already on the carrier than would be possible if the patterned components were screen printed onto the carrier.

Demonstration

There were two particular questions that the tape overcasting experiment was intended to answer. The first was whether a patterned deposition of metal powder, which contains no binder, would retain its pattern during the tape casting operation, or whether casting the tape over the deposition would wipe out the pattern. The second question was whether the binder from the tape casting slurry would penetrate into the metal powder deposition, incorporating it into the tape, and allowing the two component tape to be peeled cleanly from the glass carrier.

To test this concept, a glass plate was used as a tape casting substrate. An area of the plate was coated with a sputtered platinum electrode and 25 μm lines were scribed into the electrode. Depositions of 1.0 to 2.5 μm were made onto the glass surface by continuous application of a 300 V/cm electric field for 30 to 90 s. Deposition thickness was determined by weight gain of the glass substrate and later confirmed by direct scanning electron microscopy (SEM) examination of the green tape cross section. A 75 μm thick barium titanate tape was cast over the deposition using a traveling slip hopper with doctor blade.

The results are shown in Fig. 11. Fig. 11a shows the generally rectangular Ag/Pd deposition area on the glass carrier with vertical line pattern at the top edge. Fig. 11b shows the cast tape as it is peeled off the carrier. The top half of the picture shows the bottom of the cast tape as it is peeled up. The bottom half of the picture is a reflection of the rolled up tape off the glass carrier. The gray is the metal powder deposition incorporated into the white barium titanate tape. The pattern of lines scribed in the deposition electrode is still clearly visible as white barium titanate lines between gray areas of the metal deposition.

5.2.3. Deposition and lamination of a conductor pattern

Patterned components can also be incorporated into a multilayer by direct lamination of a patterned deposition to the stack. A patterned deposition electrode is created on a carrier and a particulate material is deposited on this pattern. Then the carrier is placed on the laminate stack, heated and pressed to incorporate the patterned deposition into the laminate. After lamination the carrier film with the conductive pattern can be peeled off and reused without needing to recreate the conductive pattern. This procedure is illustrated in Fig. 12. The layers between the patterned layers formed by EPD can be tapes cast by standard methods. The deposition can either be infiltrated with binder before lamination or can be laminated dry allowing excess binder to flow from the layer below it, bonding the deposited material.

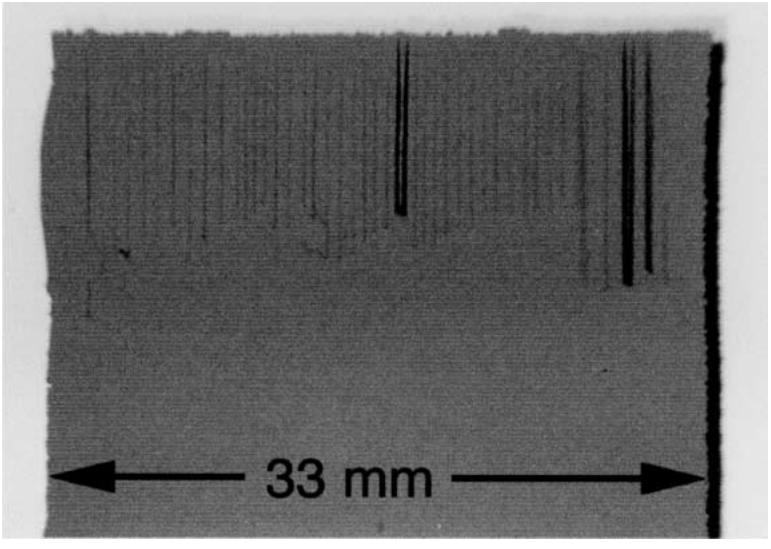

(a)

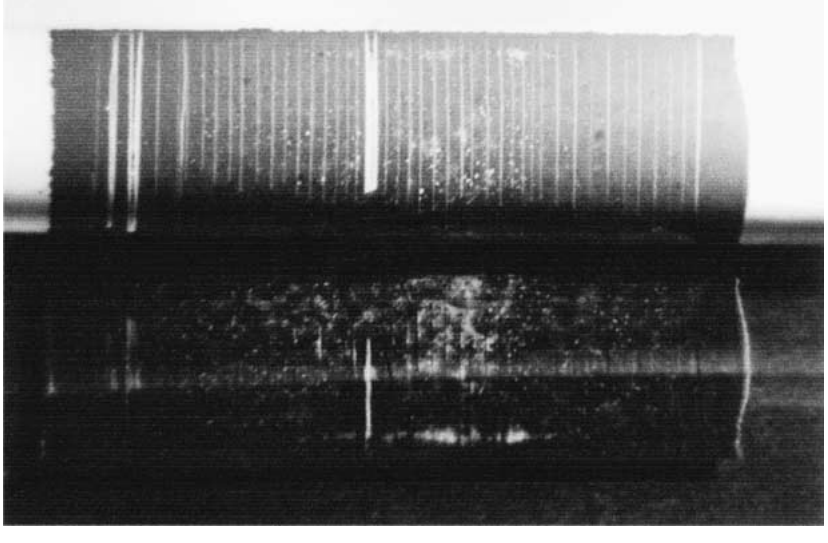

(b)

Figure 11 (a) 2.5 μm thick patterned deposition of Ag/Pd powder on a glass tape casting substrate and (b) Peel up of a barium titanate cast tape incorporating the patterned Ag/Pd deposition.

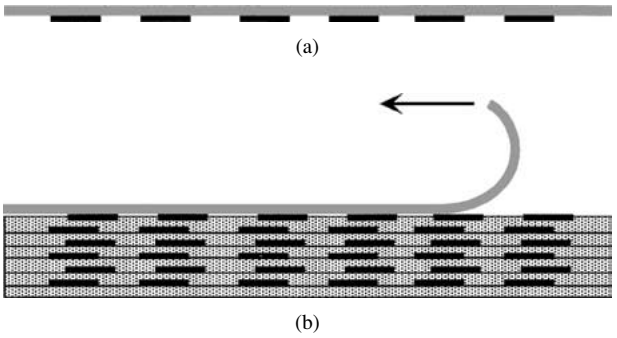

(a)

(b)

Figure 12 (a) Carrier with patterned deposition of material and (b) Carrier film is peeled off after lamination of the patterned deposition to the stack.

The advantage of using EPD in this process is the incorporation of secondary components into a laminate stack with better particle packing, lower thickness and finer detail sizes than is possible with other printing techniques.

Demonstration

The first step for this demonstration was the preparation of a patterned deposition electrode on a polyester film. A resolution test pattern shadow mask was created by electron beam lithography at the Penn State Nanofabrication Facility. This resolution test pattern includes details from 50 μm down to 1 μm.

Polyester tape casting film was cleaned by wiping with optical quality tissue, alcohol and acetone to remove any coatings or contamination on the surface. The film was spincoated with a UV photopolymer mask and exposed through the shadow mask in contact mode. The unexposed photopolymer was rinsed off exposing a patterned area of bare polyester. The entire surface is then sputter coated with platinum. The photomask and overlying platinum were removed by sonication in alcohol. Well defined conductive lines down to 2 μm were achieved with relatively little effort.

A layer of Ag/Pd powder approximately 1 μm thick was deposited on the pattern by pulsing the voltage field 3 s on/3 s off for 90 s at 150 V/cm. The deposition was

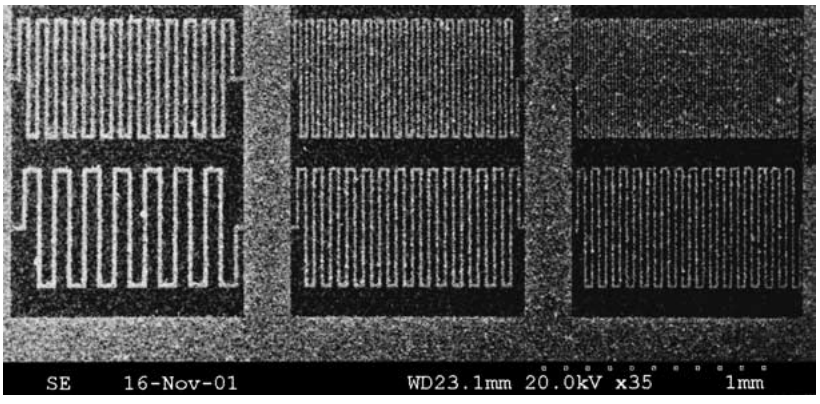

Figure 13 DuPont 951-A LTCC tape with electrophoretically formed pattern laminated to the surface. Deposition electrode pattern line widths are 15, 10 and 5 μm. Powder deposition grows $\approx$2 μm beyond edge of deposition electrode edge. Graininess of image is due to porosity of the green tape.

rinsed in a beaker of as-received acetic acid and allowed to dry. The carrier with the deposited powder was placed face down on to the shiny side of a stack of Dupont 951-A LTCC dielectric tape. This was laminated for 10 min at 200 MPa and 70°C. The polyester film carrier was peeled off the tape stack leaving the deposited Ag/Pd pattern as shown in Fig. 13.

It is worth noting that the sputtered platinum showed remarkably good adhesion to the polyester film. No damage to the deposition electrode pattern was visible due to the initial sonication or in subsequent cleaning following deposition and lamination.

The widths of the lines on the deposition electrode pattern are 15, 10 and 5 μm. During deposition the powder deposit grows both laterally as well as in thickness. Here the powder deposit has grown approximately 2 μm beyond the edge of the deposition pattern. Because of this lateral growth, features on the deposition test pattern that had less than a 5 μm spacing between them were not distinguishable. The issues of the growth of the deposition beyond the deposition pattern and their implications for pattern resolution are matters to be addressed in future publications. However, here we would like to note that the primary obstacle to higher line resolution is the tape used for lamination. This tape is typical of a commercially available low loss dielectric tape designed for LTCC processing. Designed for secondary components added at screen printing resolution, the precast tape contains alumina particles ranging in size up to 5 μm. The low uniformity of the 5 μm line shown here is due in large part to the line being the same size as particles in the tape it is being laminated to. Taking advantage of the resolution which is possible using EPD-Lamination will require the development of a new generation of LTCC materials with particle sizes in the sub-micron or preferably nanometer scale range.

5.2.4. *Multi-component deposition on a multi-electrode substrate*

The one aspect of the production of multilayer electronic devices that has not been demonstrated here is the formation of through thickness components. Currently these components are formed in an initially continuous tape by either mechanically punching or laser drilling holes into the tape. These holes are then backfilled with a second component. This process is usually restricted to tapes which are thick and strong enough to

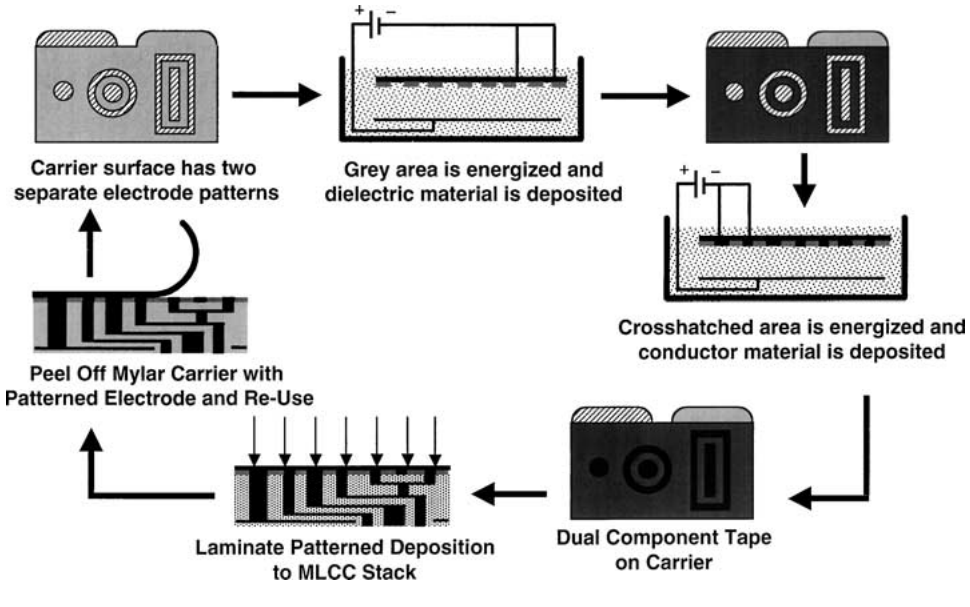

Figure 14 Forming a multicomponent tape for lamination by successive depositions on a carrier with a two part deposition electrode pattern. The pattern illustrates the forming, from left to right, of a standard circular via, a shielded via, and a shielded in-plane conductor line.

be handled off of a carrier. The smallest holes that are routinely formed and filled in this manner are 100 μm in diameter.

Multicomponent tapes with through thickness components can be formed by EPD using a carrier with a two part electrode pattern. This is illustrated in Fig. 14. The carrier would have a continuous electrode, a photopatterned polymer insulating layer, and a photopatterned top electrode. A voltage is applied to the top electrode in an EPD bath containing a dielectric powder. The deposition is rinsed and placed into a second EPD bath containing metal particles. There the second electrode is energized to produce a deposition with the same thickness as the dielectric material. This two component tape can now be laminated to a multilayer stack. The carrier with the deposition electrode pattern can be peeled off an re-used for another deposition. Because this layer is formed and handled on a carrier until lamination, the only minimum thickness limit is dictated by particle size as discussed in Section 5.2.1 above. The minimum lateral dimension of the through thickness components is a subject for future experimentation, however, a lateral dimension two times the thickness of the layer is reasonable attainable.

In addition to a dramatic reduction in scale of these components, EPD can produce shapes which are not normally possible by punching and filling. The pattern in Fig. 14 shows how a coaxial via or a shielded in-plane conductor line could be formed by EPD of multiple components. The current best practice for lateral shielding in LTCC multilayers is the punching and filling of a discontinuous row of vias connected to the ground plane to form what is called a "via fence" [18]. In contrast, EPD is able to form through thickness components as continuous lines, sharp corners, and, because the multicomponent tape is formed and handled on a carrier, cut out areas. There is no restriction that any single component be continuous to hold the tape together during processing.

6. Conclusions

This paper was begun with an example electronic material, a 70/30 silver palladium alloy 0.3 μm dia. powder, designed for co-sintering with a variety of electronic ceramics and in LTCC structures. This powder was dispersed in, and electrophoretically deposited from, a glacial acetic acid solvent. Estimation of the electrostatic stabilizing force indicates that the externally applied field used for EPD is of sufficient magnitude to overcome the interparticle repulsive force. This allows a mobile particle to come into contact with a stationary particle by electrostatic force alone. Thus for this case of EPD the growth of the deposition is attributed to the direct electrostatic force acting on each particle individually.

Using the EPD of this Ag/Pd powder we have demonstrated the formation of continuous electrode layers both sintered on a rigid substrate (constrained sintering) and within a multilayer laminate (free sintering). Based on observations of these layers the following minimum sintered thickness possible by EPD were inferred: for an electrode layer on a rigid substrate—3 to 4 times the average diameter of the starting powder; for continuous dielectric or membrane layers in a co-fired multilayer—4 times the average particle diameter; and for electrode layers in a multilayer requiring only in plane connectivity—2 times the average particle diameter.

Patterned depositions were also produced on a carrier. The minimum line width demonstrated here is 30 times the average particle diameter. The likely minimum line width possible was not determined but will in part depend on matching the particle size of the material being patterned with that of the matrix material around it.

There are several ways to incorporate this patterned deposition into a multilayer device. One method is to cast a tape over the pattern by conventional methods to form a multicomponent tape that can be removed from the carrier. An alternative method is to laminate the pattern directly to a multilayer stack, removing the carrier after lamination. A multiple component tape can also be produced by multiple depositions on a carrier with two or more electrically isolated deposition patterns. If the resulting tape is continuous then it could be removed from the carrier for stacking or the depositions could be laminated to a multilayer while still on the carrier.

The key technological point of this work is that by depositing onto a photolithographically produced pattern then transferring the deposition to a multilayer structure, the pattern can be reused. A single photolithographic operation produces a deposition pattern which can be used to electrophoretically deposit multiple parts rapidly and inexpensively. Each of these parts can have details on a dimensional scale which was previously only possible by using lithographic process for each individual part. If a set of nano-scale powders is developed which can be dispersed, electrophoretically deposited and co-sintered, this process would allow the scale of circuitry in LTCC devices to drop by more than two orders of magnitude.

Appendix

Symbols

a	Particle radius (m)
c	Molar concentration of dissolved salt (Mol/dm^3)
e	Elementary charge (1.602E-19 C)
$\mathbf{E}$	Reduced electrophoretic mobility (non-dimensional)
h	Surface to surface separation distance
k	Boltzman Constant (1.381E-23 J/K)
q	Surface charge density (C/m^2)
r	Center to center particle separation distance
T	Temperature (K)
u_{E}	Particle electrophoretic mobility (μm $\cdot$ cm/V $\cdot$ s)
z	Ion valence
ε_{o}	Permittivity of free space (8.854E-12 C^2/J $\cdot$ m)
ε_{r}	Relative dielectric constant
ζ	Particle Potential at Shear Layer (mV)
$\tilde{\zeta}$	Reduced particle potential at shear layer (non-dimensional)
η	Solvent Viscosity (Poise)
κ	Inverse Debye length (m^{-1})
ρ_{∞}	Number density of dissociated molecules of a binary salt in bulk solution (m^{-3})

References

1. M. GIERSIG and P. MULVANEY, *Langmuir* **9**(12) (1993) 3408.
2. F. HARBACH, R. NEEFF, H. NIENBURG and L. WEILER, *cfi/Ber. DKG* **67**(4) (1990) 130.
3. P. SARKAR and P. S. NICHOLSON, *J. Amer. Ceram. Soc.* **79**(8) (1996) 1987.
4. M. S. J. GANI, *Industr. Ceram.* **14**(4) (1994) 163.
5. A. BOCCACCINI and I. ZHITOMIRSKY, *Curr. Opin. Solid State Mater. Sci.* **6** (2002) 251.
6. U. KUMAR, S. F. WANG, U. SELVARAJ and J. P. DOUGHERTY, *Ferroelectrics* **154** (1994) 283.
7. R. PELTON, P. MILLER, W. MCPHEE and S. RAJARAM, *Coll. Surf.* A **80** (1993) 181.
8. J. E. LIND, JR., J. J. ZWOLENIK and R. M. FUOSS, *J. Amer. Chem. Soc.* **81** (1959) 1557.
9. B. V. WEIDNER, Ph.D. thesis, The Pennsylvania State University, 1935.
10. R. J. HUNTER, "Zeta Potential in Colloid Science, Principles and Applications" (Academic Press, New York, 1981).
11. R. W. O'BRIEN and L. R. WHITE, *J. Chem. Soc. Faraday II* **74** (1978) 1607.
12. A. L. LOEB, J. TH. G. OVERBEEK and P. H. WIERSMA, "The Electrical Double Layer Around a Spherical Colloidal Particle" (MIT Press, Cambridge, Massachusetts, 1961).
13. W. B. RUSSEL, D. A. SAVILLE and W. R. SCHOWALTER, "Colloidal Dispersions" (Cambridge Univ. Press, Cambridge, 1989).
14. V. A. PARSEGIAN and G. H. WEISS, *J. Coll. Interf. Sci.* **81** (1981) 285.
15. J. N. ISRAELACHVILLI, "Intermolecular and Surface Forces" (Academic Press, New York, 1992).
16. J. VAN TASSEL and C. A. RANDALL, *J. Eur. Ceram. Soc.* **19**(6/7) (1999) 955.
17. N. OGATA, J. VAN TASSEL and C. A. RANDALL, *Mater. Lett.* **49**(1) (2001) 7.
18. D. STEVENS and J. GIPPRICH, *Intl. J. Microcirc. Electr. Pack.* **22**(1) (1999) 43.

Received 10 January
and accepted 30 April 2003